CHEMISTRY & CHEMICAL TECHNOLOGY

Chem. Chem. Technol., 2019,
Vol. 13, No. 2, pp. 190–197

Chemistry

SUNLIGHT PHOTODEGRADABLE POLYSTYRENE-TiO_2/SiO_2 COMPOSITE

***Waed Alahmad*[1, *]**

https://doi.org/10.23939/chcht13.02.190

Abstract. Photodegradable polystyrene-catalyst (PS-TiO_2/SiO_2) composite was prepared and characterized, and its degradation under sunlight was investigated. The morphology of TiO_2/SiO_2 was amorphous with particle size of 16.6–30.1 nm and the energy gap of the catalyst was calculated. The degradation process was for 288 h, the samples under investigation were two types standard (STD) samples – a mixture of PS with catalyst, and municipal waste residues (MWR) – a combination of PS-catalyst with MWR. The degradation was measured in dark and under sunlight. The MWR samples percent degradation was higher than that of STD samples.

Keywords: methylene blue, polarized light microscopy, municipal waste residues, biodegradation.

1. Introduction

Polystyrene (PS) as a typical thermoplastic polymer, is one of the essential materials from the modern plastic industry. PS has been used all over the world, due to its excellent physical properties and low cost. It is used in many applications such as packaging, consumer electronics, construction, and medicine [1-4].

However, the accumulation of the discarded PS has led to the environmental pollution due to its non-degradability under environmental conditions.

Techniques used for PS degradation, thermal or catalytic, require high temperatures and appropriate catalysts, both of which are costly, whereas photocatalytic oxidation reactions can occur under moderate conditions, including room temperature conditions, one-atmosphere pressure, using molecular oxygen as the only oxidant.

TiO_2 as a photocatalyst has been proven to be a useful way to degrade solid polymer in open air [5-7], TiO_2 catalytically reacts with H_2O in air under sunlight exposure, producing $OH^•$ (highly reactivity species), which initiate the photodegradation of polymeric materials under mild conditions.

The degradation rate strongly depends on dispersity of TiO_2 particle in polymeric matrix [1]. The incorporation often prevents aggregation of TiO_2 nanoparticles into porous substrates such as zeolites or mesoporous silica. The porous supports enhance the local contaminant concentration and thus increase the local contaminant mass transferring from bulk to TiO_2 surface [8].

PS is used in many fields and has replaced natural resources such as cotton, wood, and metals. Its hardness, hydrophobic nature and chemical composition cause it to persist in the environment without any decomposition for an extended period, thus causing environmental pollution. As waste plastic materials have become a severe problem, recycling is receiving attention as a means of preserving the environment and reserving resources. Polystyrene waste requires the transportation of significant large volume of materials, which is costly and makes recycling economically unfeasible [9-11].

PS does not directly metabolize by microorganisms, since they cannot pass into the cell. It has been reported that prior photodegradation enhances biodegradation of non-biodegradable or even biodegradable polymers. Photodegradation results typically in oxygenated chemical bounds and shorter chains, which usually are more easily consumed by microorganisms, turning the polymer more accessible for microbial assimilation [9].

J. Puls *et al.* [10] reported that photodegradation with TiO_2 causes surface pitting of cellulose acetate polymer, increasing the material surface area, which enhances biodegradation. The combination of both photo and biodegradation allows cooperation that improves the overall degradation rate [9, 10].

The current study aims to enhance the photodegradation of PS in the solid phase under environmental conditions. TiO_2 was introduced in the liquid phase into SiO_2 nanoparticles with 25 % w/w by the impregnation method, degradation takes place under sunlight after uniform distribution of catalyst with PS.

---

[1] Chemistry Department, Faculty of Science, Ha'il University, Ha'il, Saudi Arabia
[*] *w.alahmad@uoh.edu.sa*

2. Experimental

2.1. Catalyst Preparation

Cabosil M-5 silica oxide, titanium isopropoxide ($Ti(i\text{-}OC_3H_7)_4$; 97% purity), absolute ethanol, methylene blue (MB), cyclohexane, and polystyrene ($(CH_2CH(C_6H_5))_n$; average $M_w \approx 192{,}000$) were purchased from Sigma-Aldrich; the SiO_2 was treated with water in order to condense its volume for easier handling. SiO_2/TiO_2 supported oxide catalyst was prepared by the incipient wetness impregnation of SiO_2 with an ethanol solution of titanium isopropoxide. After impregnation at room temperature, the sample was kept overnight. Removal of the solvent was performed by conventional drying, first at room temperature for 24 h and afterward at 383 K for 2 h before being calcinated for 5 h at 673 K in air. The resulting photocatalyst was then denoted as TiO_2/SiO_2.

Phase identification of the catalyst was then conducted using X-ray diffraction (XRD). Field emission scanning electron microscopy (SEM-EDS; JSM-7800F, JEOL, USA) and UV-Vis spectrophotometry using a Varian Cary Eclipse spectrofluorometer were also conducted. Absorption was carried out in a 10 cm cuvette with a Shimadzu UV-2401PC UV-Vis spectrophotometer, and excitation-emission matrices (EEMs) were generated for the sample using excitation wavelengths between 190–300 nm at 5 nm intervals and emission wavelengths of 380–700 nm in 2.5 nm intervals, with 5 nm bandwidths for the excitation and emission modes.

2.2. Preparation of the PS Catalyst Composite

At this stage, 1.5 g of PS were dissolved in 60 ml cyclohexane under vigorous stirring for 2 h to obtain the PS solution; next, 0.060 g (4 wt %) and 0.120 g (8 wt %) of catalyst powder were suspended uniformly in the above-mentioned 60 ml solution to obtain the PS catalyst composite. An aliquot of 10 ml PS-TiO_2/SiO_2 solution was spread on a glass plate (***R*** = 4.5) and dried for 30 min at 353 K before being dried for 48 h at room temperature.

The photocatalytic degradation of the PS-TiO_2/SiO_2 films was then investigated under sunlight irradiation for 288 h. The degradation of the films was evaluated directly from their weight loss. Fourier transform infrared spectrophotometry (FTIR; Perkin-Elmer 843, ATR sample holder) was used to study characteristic spectra of the films before and after irradiation. The measurement range was 500–4000 cm^{-1}, with 4 cm^{-1} resolution and 0.475 cm^{-1}/s scanning speed. Polarized light microscopy (PLM) was also used to investigate the surface of the films before and after sunlight irradiation. The films were analyzed using an NMAFA Zeiss Axioplan Pol Universal polarized light microscope using transmitted light in a bright field and crossed polarization with the magnification range of 100–1000×.

2.3. Photocatalytic Activity of the MB Solution: Photodegradation under UV Illumination

MB was used as a model compound to express the photocatalytic activity of TiO_2; 10 mg/l of MB with 0.2 % catalyst TiO_2/SiO_2 was used in the study. The sample was illuminated using a 50 W xenon lamp (Electro-Technic Products, USA) for 180 min at 10 cm distance using magnetic stirring. Degradation was measured using a UV-VIS double-beam spectrophotometer (Model UVD-2950) at the incident wavelength of 665 nm. The spiked sample was 200 ml of deionized water with 10 mg/l of MB. Each 30 min a 5 m sample was taken, then centrifuged (4000 rpm, 3 min) and analyzed using UV spectrophotometer.

3. Results and Discussion

3.1. Characterization of TiO_2/SiO_2 by SEM, EDX, and XRD

Fig. 1 shows the characterization of the catalysis. The particle size and morphology were both confirmed by SEM analysis. The SEM image shows many spheres-like nanoparticles with various caves and heaves, which mainly resulted from the aggregates of nano TiO_2 over SiO_2. A slight agglomeration was also observed. EDX analysis for the sample (Table 1) confirmed the presence of elements corresponding to SiO_2 (81.69 %) and TiO_2 (18.31 %). SEM image shows the particle size between 16.6–30.1 nm.

Table 1

EDX analysis giving atomic percent for TiO_2/SiO_2

Element	Weight %	Atomic %	Compd %	Formula
Si	38.19	28.27	81.69	SiO_2
Ti	9.39	5.06	18.31	TiO_2
O	52.42	66.67	–	–

XRD pattern of the catalyst shows an amorphous structure for the TiO_2/SiO_2. The large broad peak at $2\theta =$ $= 22°$ represents Si. Titanium has $2\theta = 38°$, 48°, and 55°; (004), (200), (105) planes of anatase titania, respectively. The morphology of the catalyst is considered as an amorphous structure; there should be a peak at $2\theta = 25.5$ (101) plane, which is shielded with the large broad peak of Si [11]. Several studies have reported that XRD hardly detects if the presence of TiO_2 crystallites is below 30 % of TiO_2 loading [12-14].

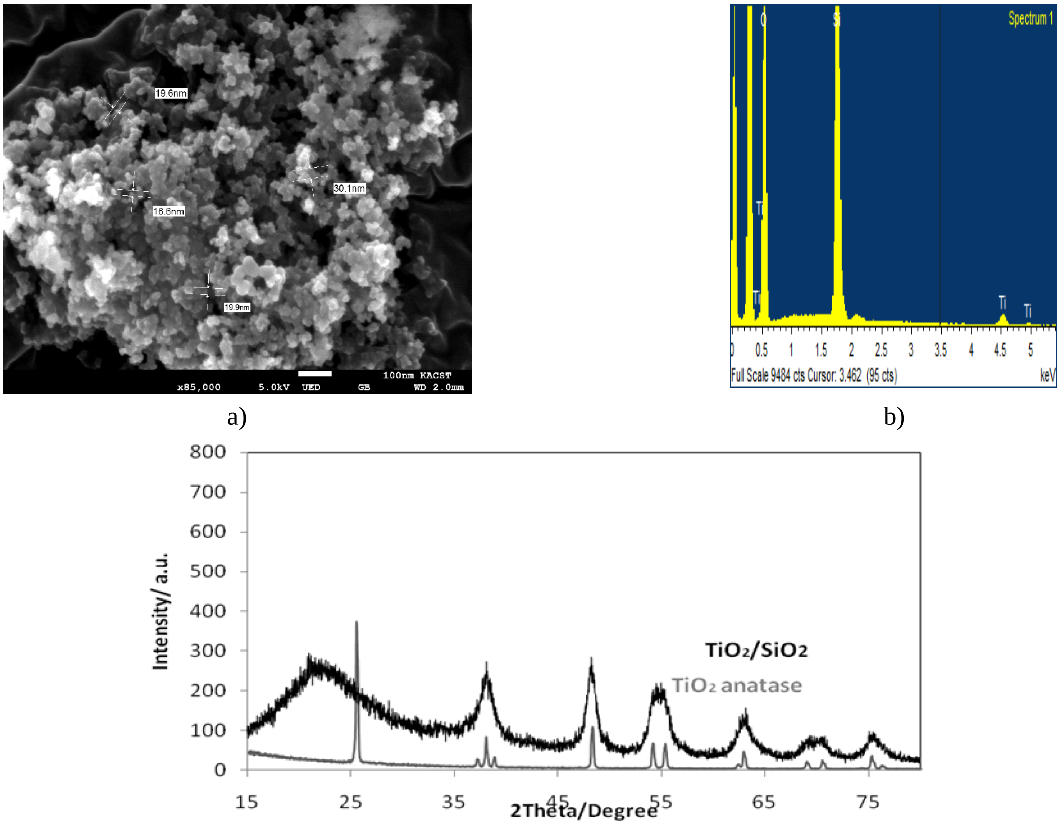

a) b)

c)

Fig.1. Characterization for TiO_2/SiO_2: SEM image (a) showing the particle size (point analysis); EDX analysis (b) confirming the presence of Si, Ti, and O; XRD results (c) as amorphous structure material, (TiO_2 anatase is used as reference)

Matsumura *et al.* [15] and Jia *et al.* [16] found that the catalyst with amorphous morphology shows a higher activity for degradation and selectivity than crystalline one [15, 16].

3.2. UV-Vis Spectroscopy; Energy Gap Calculation

Fig. 2 shows the emission wavelengths for the catalyst after being excited. The excitation-emission matrices (EEMs) were generated for the sample using excitation wavelengths of 190–300 nm at 5 nm intervals and emission wavelengths of 380–700 nm at 2.5 nm intervals, with 5 nm bandwidths for the excitation and emission modes, the λ_{em} for the TiO_2/SiO_2 were 363 and 378 nm.

The significance of the band gap is the determination of the solar spectrum portion the catalyst will absorb to initiate the degradation process. The UV-Vis spectrum can be used to calculate the band gaps of semiconductor material for several transitions (allowed direct, allowed indirect, forbidden direct, and forbidden indirect), by plotting the graph between $(ah\nu)^{1/n}$ *vs.* photon energy hn (Tauc's method), where a is the optical absorption coefficient; the power factor n = 0.5, 2, 1.5 and 3.

Another method for calculating E_g is directly from the equation $E=\frac{hc}{l}$. Substituting the constants h (Plank's constant) and c (speed of light) in the equation, the energy band gap $E=\frac{1240.8}{l}$ nm.

Calculating E_g from Fig. 2, which represents the emission wavelength *vs.* intensity, we obtain E_g = 3.42 eV at λ = 363 nm equals and E_g = 3.28 eV at λ = 378 nm. UV irradiation is needed in semiconductor to start the degradation of organic compounds; the band gap comes between 3.4–3.1 eV for the initiation of the photo process. TiO_2 band gap energy is shifted to the red region of the electromagnetic spectrum by doping with metal, carbon, sulfur, and nitrogen. Eventually, doped or undoped, titanium dioxide is the photocatalyst to which the largest number of studies has been devoted [17, 19].

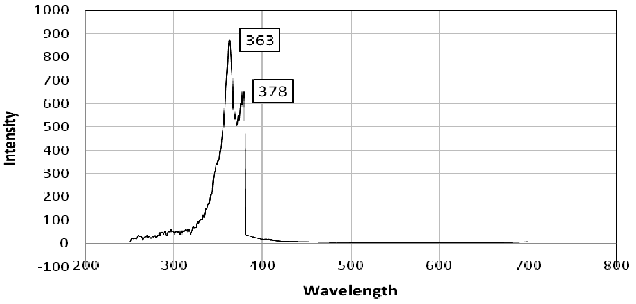

Fig. 2. Emission wavelengths for TiO$_2$/SiO$_2$ after excitation λ from 190–300 nm and emission λ from 380–700 nm

3.3. Photocatalytic Activity Evaluation: MB Photodegradation

The initial and equilibrium dye concentrations were determined using a calibration curve based on absorbance at $\lambda_{\max}$ = 665 nm *vs.* dye concentration in the standard dye solutions. In order to construct a calibration curve (Fig. 3), MB concentrations of 0.5, 1.0, 3.0, 5.0, 7.0, 10.0, 15.0, and 20.0 mg/l were prepared in volumetric flasks. The absorbance of each of the standard MB solutions was measured at the maximum absorption wavelength of 665 nm [7, 8]. The sample was illuminated using a 50 W xenon lamp (Electro-Technic Products, USA) for 180 min at 10 cm distance using magnetic stirring. Degradation was measured using a UV-Vis double-beam spectrophotometer (Model UVD-2950) at the incident wavelength of 665 nm. Degradation efficiency under UV illumination was calculated as:

$$\textit{Degradation efficiency} = \frac{C_0 - C_i}{C_0} \cdot 100\% \qquad (1)$$

where C_0 is initial concentration and C_i is a sample concentration.

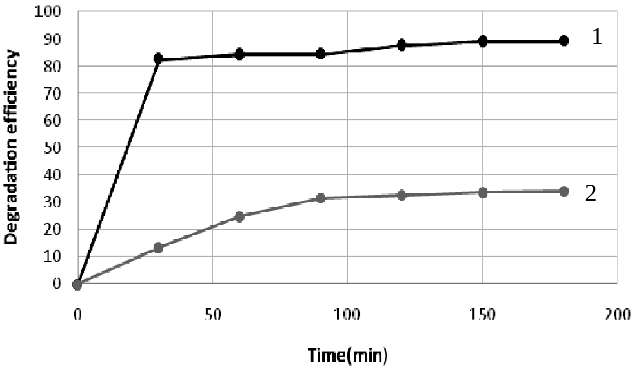

Fig. 3. Degradation efficiency of MB under UV illumination (1) and in dark (2) for estimating the photoactivity of TiO$_2$/SiO$_2$

Degradation efficiency for TiO$_2$/SiO$_2$ under UV = 89.25%, while in dark reached 34.05%.

3.4. FTIR: Characterization of PS-TiO$_2$/SiO$_2$ Degradation

Fig. 4 shows the spectrum for TiO$_2$ (commercial anatase), SiO$_2$ (Cabosil M-5), and TiO$_2$/SiO$_2$. The labeled peaks at 1068 and 805 cm^{-1} are attributed to Si-O-Si band asymmetric stretching vibrations in both bare SiO$_2$ and TiO$_2$/SiO$_2$. The peak around 1631 cm^{-1} is assigned to the bending vibration of OH bond, due to the chemisorbed water. Peak around 3415 cm^{-1} is ascribed to the stretching mode of OH bond and related to free water, OH peaks are found in bare SiO$_2$ and bare TiO$_2$, whereas for TiO$_2$/SiO$_2$ there are no peaks indicating the presence of OH. The labelled peaks for TiO$_2$ anatase at 942 and 741 cm^{-1}, and no peaks of TiO$_2$ in the TiO$_2$/SiO$_2$ were found. The band around 1400 cm^{-1} is assigned to the Ti–O–Ti stretching mode in bare TiO$_2$, and there is no peak around 910–960 cm^{-1} region which corresponds to the Ti–O–Si bonds. The reason is the high percentage of SiO$_2$ (75 %) comparing to TiO$_2$ (25 %), overlap of the peak with the large broad peak of SiO$_2$ at 1063 cm^{-1} [20, 21].

Fig. 5 shows the spectra before and after sunlight irradiation of the PS-TiO$_2$/SiO$_2$ composite films. The characteristic peaks of the phenyl rings were found at 1492, 1451, 751, and 698 cm^{-1} (peaks for pure PS) [22]. The phenyl ring opening reaction in PS is observed from the high decrease in the intensity of the aromatic peaks at 751 and 698 cm^{-1}. The peaks appeared at 2352 and 3776 cm^{-1} are related to phenyl –C=O stretching, and O–H vibration modes, respectively. We observe an increase in the intensities of the carbonyl peak in the PS-TiO$_2$/SiO$_2$ composite as compared to pure PS.

UV affects PS which leads to chemical changes within the polymeric chains, and results in the formation of several functional groups. Irradiation of PS in the presence of oxygen can lead to the production of carbonyl and hydroxyl group moieties; initial degradation of PS leads to a radical [–CH$_2$CH(Ph)]. Such radicals can abstract a proton from other polymeric chains to produce various other radicals [CH$_2$C(Ph)–CH$_2$–, CH$_2$C(Ph)–CH$_3$– and CH$_2$CHC(H)–CH(Ph)–]. These radicals react with oxygen to produce the corresponding peroxy radicals. Therefore, the changes in the IR spectrum of PS due to irradiation can be used as a measure of photodegradation within the polymeric materials [22].

The mechanism for the degradation of polymers by heterogeneous photocatalysis involves the generation of singlet oxygen and hydroxyl radical, after the excitation of the catalyst the production of electron-hole combination takes place, the degradation being initiated by hydroxyl radical. The greatest advantage of photocatalytic degradation is complete mineralization for organic pollutants. The most advantage of photodegradation is the complet minirilization for the pollutant. The degradation of polystyrene starts from the dehydrogenation step until it reaches CO$_2$ evolution [23-25]. The scheme below illustrates the photodegradation process [23-25].

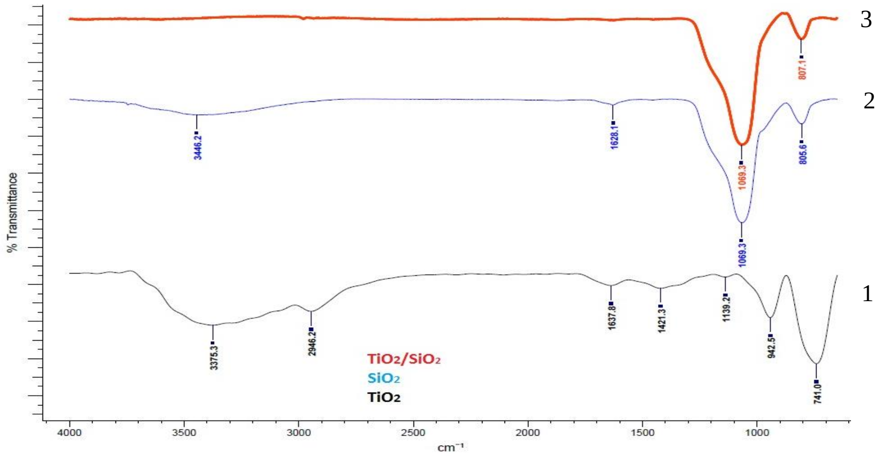

Fig. 4. FTIR spectrums for TiO_2 (commercial anatase, (1)), SiO_2 (Cabosil M-5, (2)), and TiO_2/SiO_2 (3)

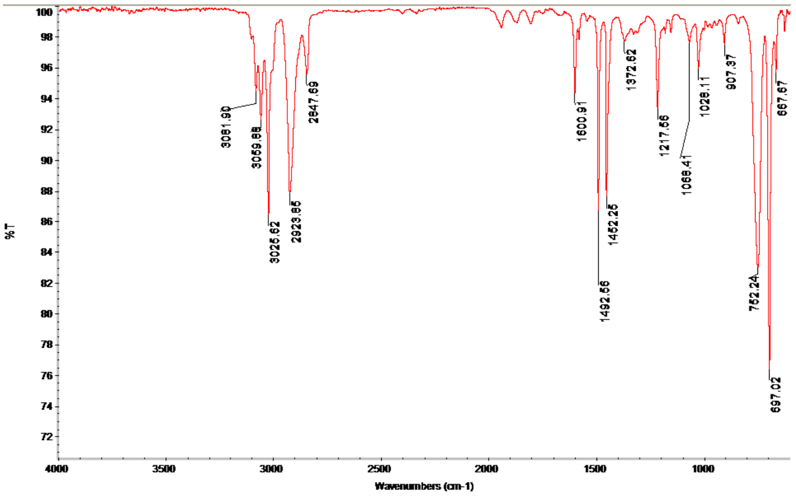

a)

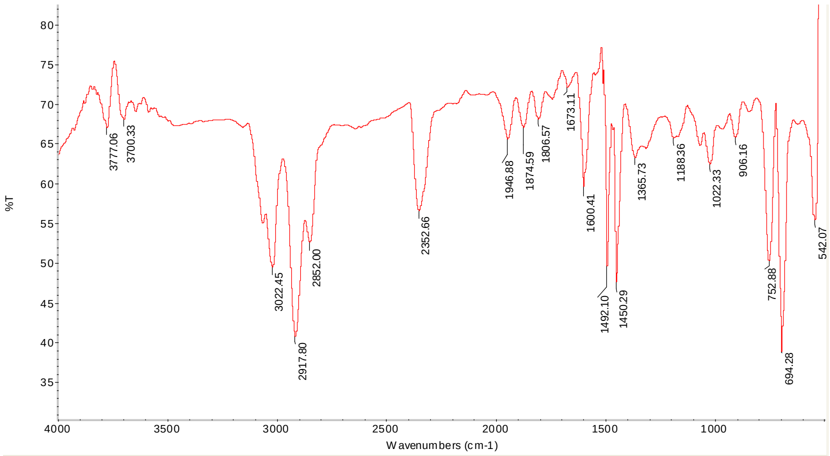

b)

Fig. 5. FTIR spectra of PS-TiO_2/SiO_2 before (a) and after (b) sunlight irradiation for 288 h

On the other hand, the results of this investigation provide a valuable methodology to produce highly efficient and controllable photodegradable plastics.

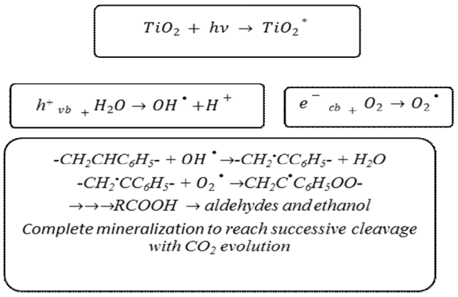

$$TiO_2 + h\nu \rightarrow TiO_2^{*}$$

$$h^{+}{}_{vb} + H_2O \rightarrow OH^{\bullet} + H^{+}$$

$$e^{-}{}_{cb} + O_2 \rightarrow O_2^{\bullet}$$

$$\text{-}CH_2CHC_6H_5\text{-} + OH^{\bullet} \rightarrow \text{-}CH_2{}^{\bullet}CC_6H_5\text{-} + H_2O$$

$$\text{-}CH_2{}^{\bullet}CC_6H_5\text{-} + O_2^{\bullet} \rightarrow CH_2C^{\bullet}C_6H_5OO\text{-}$$

$$\rightarrow\rightarrow\rightarrow RCOOH \rightarrow \text{aldehydes and ethanol}$$

Complete mineralization to reach successive cleavage with CO_2 evolution

3.5. Weight Loss of PS-TiO$_2$/SiO$_2$ Degradation

The PS-TiO$_2$/SiO$_2$ composite films were weighed every 24 h, for a total time of 288 h under sunlight. The preparation of the composite films is mentioned in experimental part; two types of samples were used to study the degradation process: the first ones – standard (STD) samples (PS with catalyst) and second ones – municipal waste residues (MWR) samples (PS with catalyst and 0.5 g of homogenous MWR). Municipal waste is defined as waste collected and treated by or for municipalities [24]. It was collected from landfill Hail region (it covers waste from household waste as well as yard and garden waste). Fig. 6 shows Hail location in KSA [26], municipal waste residue samples consisted of moisturized soil with partially decomposed waste.

The degradation rate strongly depends on dispersity of catalyst particle in PS matrix. The loading method was by melting the PS and vigorous mixing of the solution, SiO$_2$ was used to enhance the dispersion of TiO$_2$ in the PS composite due to the poor dispersity of TiO$_2$ particle in hydrophobic matrix.

Table 2 gives the percent weight loss *vs.* time, according to Eq. (2):

$$Weight\ loss = \frac{W_0 - W_i}{W_0} \cdot 100\% \qquad (2)$$

where W_0 is the initial sample weight, and W_i is the sample weight.

Degradation of the films in the dark, in both 4 wt % and 8 wt % (weight of catalyst to the PS weight) was around 12 % (Table 2). PS as all polymers is weathered due to environmental factors such as light and temperature. When PS is subjected to UV irradiation in the presence of air, it undergoes a rapid yellowing and gradual embrittlement (aging), and losses its mechanical and tensile properties.

The degradation percent increased as the amount of catalyst doubled, in all samples, the MWR degradation was higher than STD samples, with 61 % degradation.

PS is used in many fields and has replaced natural resources. Its hardness, hydrophobic nature and chemical composition cause it to persist in the environment without any decomposition for an extended period, thus leading to environmental pollution. Photodegradation enhances the initiation of biodegradation where photodegradation results typically in shorter chains, which usually are more easily consumed by microorganisms, turning the polymer more accessible for microbial assimilation [9].

Liu *et al.* [25] reported a degradation percent of 12.6 % of the PE-B-goethite film under UV, while Thomas *et al.* [7] reported 18.1 % weight loss for PE film containing TiO$_2$-50 and 16 % weight loss has been recorded with PS-ZnO under UV [23]. Lei *et al.* [24] reported 9.53 % weight loss for PS-TiO$_2$ films and 19.89 % for PS-HADPG-TiO$_2$ films under sunlight (a hindered amine-modified aromatic polyamide dendrimer/ polystyrene-grafted-TiO$_2$ hybrid).

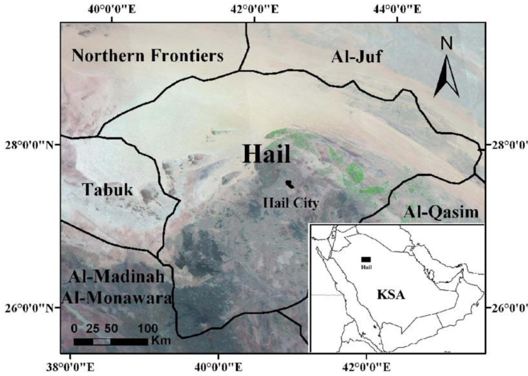

Fig. 6. Hail region location (KSA), a MODIS image [26]

Table 2

Weight percent degradation in the dark and under sunlight

Time, h	4 % Dark	4 % Sun STD	4 % Sun MWR	8 % Dark	8 % Sun STD	8 % Sun MWR
0	0	0	0	0	0	0
48	11.26	12.44	18.24	5.21	10.52	12.95
96	11.95	16.04	18.57	10.64	11.50	15.05
144	11.95	34.69	33.16	10.64	37.79	34.99
192	12.01	50.40	44.77	11.01	49.62	51.79
240	12.56	52.20	50.10	11.58	52.80	55.90
288	12.99	54.00	55.71	12.38	55.86	61.58

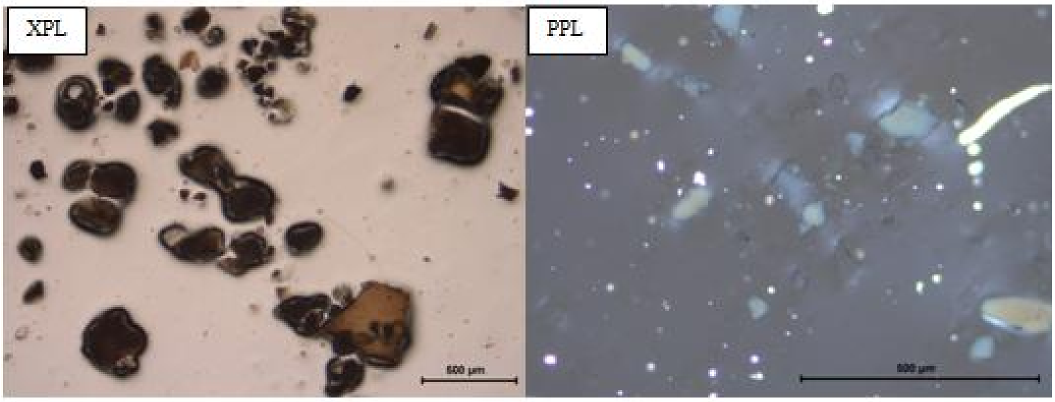

Fig. 7. Surface morphologies of PS-TiO_2/SiO_2 thin films before irradiation

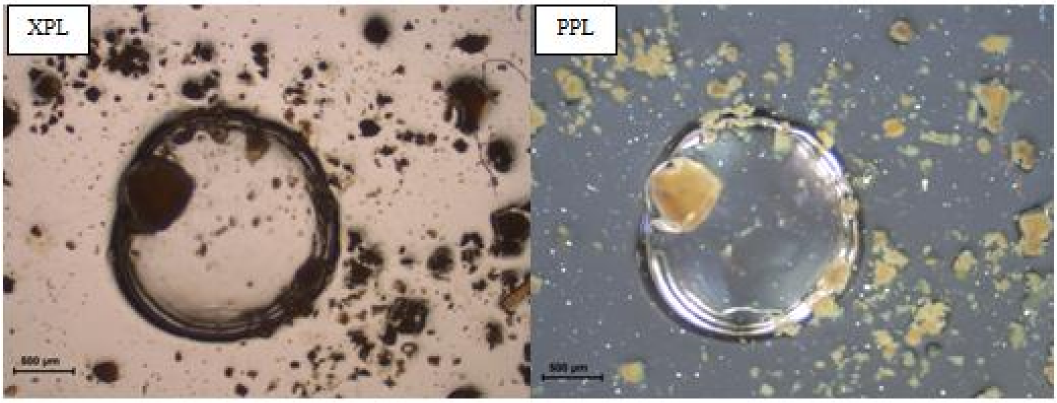

Fig. 8. Surface morphologies of PS-TiO_2/SiO_2 thin films after irradiation

3.6. Surface Morphologies of Thin PS-TiO_2/SiO_2 Film by PLM

The use of polarized light is a contrast-enhancing technique that improves the quality of the image obtained with birefringent materials. Primarily employed in crystallography, this technique represents a complicated subject that is usually restricted to the fields of geology, mineralogy, and chemistry. Steady advances that have been made over the past few years, however, have enabled biologists to study the birefringent character of many anisotropic sub-cellular assemblies.

Figs. 7 and 8 show the surface morphologies of thin PS-TiO_2/SiO_2 films before and after irradiation using PLM with two modes: plane-polarized light (PPL) and cross-polarized light (XPL). Two types of materials were found in the samples: material with a pale yellow, smooth surface and small particles representing fully dissolved and some undissolved PS, whereas the black and grey coloured material represented the catalyst TiO_2/SiO_2 in the PPL. For the XPL, the color scheme was reverse.

Before irradiation, the surface was smooth and adhered to the glass. After irradiation, the film exhibited cracks and air bubbles, with no PS adhering to the glass surface. It appears that the photocatalytic reaction initially starts at the interface between the PS exposed catalysts, which leads to the formation of cavities centered on the catalyst particles. The holes increase with irradiation, simultaneously extending to the inner film and spreading over the film surface [19, 27].

The degradation rate strongly depends on dispersity of catalyst particle in a polymeric matrix. Herein the loading method was used is solution mixing of polymeric materials and catalyst. An improvement of the mixing method has been required due to poor dispersity of hydrophilic TiO_2 particle in hydrophobic matrix [1].

4. Conclusions

PS-TiO_2/SiO_2 was prepared, characterized, and the percent degradation of the composite film under sunlight for 288 h was measured by FTIR and weight-loss percentage before and after exposure. The degradation of STD samples and MWR samples was measured; the degradation percent increased as the amount of catalyst doubled in all samples; the MSR degradation was higher than STD samples, with 61 % degradation. PS persists decomposition causing environmental pollution. Photodegradation enhances the initiation of biodegradation. Replacement of a photodegradable PS gives the opportunity to decrease the pollution with PS by enhancing the degradation process, both the photo (as initiation) and then the biodegradation in the solid polymers under sunlight irradiation.

Acknowledgments

This work was supported by grants from King Abdulaziz City for Science and Technology KACST (LGP-35-105).

References

[1] Nakatani H., Kawajiri G., Miyagawa S., Motokucho S.: Polym. Degrad. Stab., 2016, **130**, 135. https://doi.org/10.1016/j.polymdegradstab.2016.06.012
[2] Yousif E., Haddad R.: Springer Plus, 2013, **2**, 1. https://doi.org/10.1186/2193-1801-2-1
[3] Shang J., Chai M., Zhu Y.: J. Solid State Chem., 2003, **174**, 104. https://doi.org/10.1016/S0022-4596(03)00183-X
[4] Hu X., Chen F., Li N. *et al.*: Polym. Degrad. Stab., 2017, **142**, 55. https://doi.org/10.1016/j.polymdegradstab.2017.05.014
[5] Wenyao L., Ying L., Shuang S. *et al.*: Polym. Degrad. Stab., 2013, **98**, 1754. https://doi.org/10.1016/j.polymdegradstab.2013.05.027
[6] Thomas R., Sandhyarani N.: RSC Adv., 2013, **3**, 14080. https://doi.org/10.1039/c3ra42226g
[7] Thomas R., Vaishakh N.,Sandhyarani N.: Colloid. Surf. A, 2013, **422**, 1. https://doi.org/10.1016/j.colsurfa.2013.01.017
[8] Verbruggen S.: J. Photochem. Photobiol. C, 2015, **24**, 64. https://doi.org/10.1016/j.jphotochemrev.2015.07.001
[9] Sadi R., Fechine G., Demarquette R.: Polym. Eng. Sci., 2013, **53**, 2109. https://doi.org/10.1002/pen.23471
[10] Puls J., Wilson S., Holter D.: J. Polym. Environ., 2011, **19**, 152. https://doi.org/10.1007/s10924-010-0258-0
[11] Ekou T., Especel C., Royer A.: Catal. Today, 2011, **173**, 44. https://doi.org/10.1016/j.cattod.2011.05.016
[12] Fa W., Zan L., Gong C. *et al.*: Appl. Catal. B-Environ., 2008, **79**, 216. https://doi.org/10.1016/j.apcatb.2007.10.018
[13] Ma L., He D.: Top. Catal., 2009, **52**, 834. https://doi.org/10.1007/s11244-009-9231-3
[14] Lanza R., Järas G., Canu P.: Appl. Catal. A, 2007, **325**, 57. https://doi.org/10.1016/j.apcata.2007.03.005
[15] Matsumura H., Higashimine K., Koyama K., Ohdaira K.: J. Vac. Sci. Technol. B, 2015, **33**, 1201. https://doi.org/10.1116/1.4915494
[16] Jia H., Stark J., Zhou L. *et al.*: RSC Adv., 2012, **2**, 10874. https://doi.org/10.1039/c2ra21993j
[17] López R., Gómez R.: J. Sol-Gel Sci. Technol., 2012, **61**, 1. https://doi.org/10.1007/s10971-011-2582-9
[18] Souza L., Shree S., Balakrishna G.: Ind. Eng. Chem. Res., 2013, **52**, 16162. https://doi.org/10.1021/ie402592k
[19] GuoT., Pakhomov G., Wen T. *et al.*: Jpn. J. Appl. Phys., 2006, **45(49)**, 1314.
[20] Kannaiyan D., Kochuveedu S., Jang H. *et al.*: Polymers, 2010, **2**, 490. https://doi.org/10.3390/polym2040490
[21] Mungondori H., Tichagwa L., Green E.: Br. J. Appl. Sci. Technol., 2015, **5**,447. https://doi.org/10.9734/BJAST/2015/11049
[22] Ali G., El-Hiti G., Tomi I. *et al.*: Molecules, 2016, **21**, 1699. https://doi.org/10.3390/molecules21121699
[23] Mohamed R.R. In book: Springer Reference Live; Polymers and Polymeric Composites: A Reference Series. Publisher: Springer, Editors: Sanjay Palsule. Fillers for Polymer Applications, Rothon R 2017 ISSN:2510-3458
[24] Lei Y., Lei H., Huo J.: Polym. Degrad. Stab., 2015, **118**, 1. https://doi.org/10.1016/j.polymdegradstab.2015.04.005
[25] Yousif E., Haddad R., El-Hiti G., Yusop R.: J. Taibah Univ. Sci., 2017, **11**, 97.
[26] Hereher M., Al-Shammari A., Abd Allah S.: IJG, 2012, 3(02), 349. https://doi.org/10.4236/ijg.2012.32038
[27] Kamrannejada M., Hasanzadeha A., Nosoudib N. *et al.*: Mater. Res., 2014, **17**, 1039. https://doi.org/10.1590/1516-1439.267214

Received: January 17, 2018 / Revised: February 26, 2018 /
Accepted: June 23, 2018

ФОТОДЕГРАДАЦІЯ КОМПОЗИТУ НА ОСНОВІ ПОЛІСТИРОЛ-TiO_2/SiO_2 ПІД ДІЄЮ СОНЯЧНОГО СВІТЛА

Анотація. *Одержано і охарактеризовано фотодеградабельний каталізатор-композит ПС-TiO_2/SiO_2 та вивчено його деградацію під дією сонячного світла. Встановлено аморфну структуру TiO_2/SiO_2 з розміром частинок від 16,6 до 30,1 нм. Розраховано енергетичну зону каталізатора. Дослідження деградації проводили протягом 288 годин на двох зразках: суміші ПС з каталізатором (STD) і комбінації ПС-каталізатора з міськими відходами (MWR). Деградацію визначено в темряві та під дією сонячного світла. Встановлено, що відсоткова деградація зразків MWR є вищою у порівнянні з STD зразками.*

Ключові слова: *метиленовий синій, поляризована світлова мікроскопія, муніципальні відходи, біодеградація.*